Synthesis of Electromagnetic Functionalized Nickel/Polypyrrole Core/Shell Composites

ARTICLE *in* THE JOURNAL OF PHYSICAL CHEMISTRY B · SEPTEMBER 2008

Impact Factor: 3.3 · DOI: 10.1021/jp804327k · Source: PubMed

8 AUTHORS, INCLUDING:

Ping Xu
Harbin Institute of Technology
101 PUBLICATIONS **2,926** CITATIONS

SEE PROFILE

Synthesis of Electromagnetic Functionalized Nickel/Polypyrrole Core/Shell Composites

Ping Xu,[†] Xijiang Han,*[,†] Chao Wang,[†] Donghua Zhou,[†] Zushun Lv,[†] Aihua Wen,[†] Xiaohong Wang,[‡] and Bin Zhang[†]

Department of Applied Chemistry, Harbin Institute of Technology, Harbin 150001, China, Beijing Institute of Aeronautical Materials, Beijing 100095, China

Received: May 16, 2008; Revised Manuscript Received: June 17, 2008

Microstructured Ni/PPy (PPy: polypyrrole) core/shell composites were prepared from an in situ chemical oxidative polymerization of pyrrole (Py) monomer in the presence of Ni powder, with ammonium persulfate (APS) as oxidant and citric acid ($C_6H_8O_7$) as dopant. X-ray diffraction and Fourier transform infrared analyses indicate that there is no chemical interaction between Ni powder and protonated PPy. The mass percentages of PPy, calculated from the remanent weight percentages of Ni/PPy composites after thermogravimetric analysis, are in consistent with those as designed. The prepared Ni/PPy composites are soft and ferromagnetic materials, where a linear increase of saturation magnetization (M_S) and remanent magnetization (M_R) as a function of Ni powder content is proposed. The permeability of Ni/PPy composites presents a natural magnetic resonance at 6.0 GHz, and Cole−Cole semicircle was applied to explain the permittivity. Electromagnetic absorption less than −10 dB is found for Ni/Py = 4:1 (11−15.4 GHz) and Ni/Py = 2:1 (12−17.5 GHz). The ternary Debye relaxations for enhanced dielectric loss induced by PPy coatings and proper electromagnetic impedance matching due to the synergetic consequence of the Ni cores and PPy shells contribute to the improvement of the electromagnetic absorption of the Ni/PPy core/shell composites. It is important to notice that dielectric loss and electrical conductivity should be considered simultaneously in designing dielectric-type electromagnetic absorbing materials.

Introduction

Organic−inorganic composites with an organized structure usually provide a new functional hybrid, with synergetic or complementary behavior between organic and inorganic materials, which have attracted considerable attention for their potential applications.[1,2] The desire to create structures that combine the mechanical flexibility, optical properties, and electrical properties of conducting polymers with the high electrical conductivity and magnetic properties of metals has inspired the development of several techniques for the controlled growth of composites of metals and polymers.[3−7] In recent years, there has been a tremendous increase in interest in materials that are both magnetic and electrically conductive, which have potential applications such as electromagnetic shielding (EMS), molecular electronics, nonlinear optics, microwave absorption, and catalysis.[8,9] Among those multifunctionalized micro/nanostructures, electromagnetic functionalized micro/nanostructures of conducting polymers are of special interest due to their potential applications in EMS and microwave absorbing materials. Several groups have reported the electromagnetic functional micro/nanostructures of conducting polymers related materials.[10−12] Polypyrrole (PPy) has provided the possibility of being a good microwave absorbent because of its controllable dielectric loss ability, ease of preparation, good environmental stability, and the embedment of nanoparticle (NP) cores inside the conducting PPy is of interest because of the strong electronic interaction between the NPs and polymer matrices.[13,14]

Molecular structure of the electrical and magnetic component in micro/nanostructured composites will affect the electromagnetic properties of the micro/nanostructured composites. In our previous works, by supplying $BaFe_{12}O_{19}$ (BF) NPs as nucleation sites, the produced polyaniline (PANI)/BF and PPy/BF nanocomposites have alternative electrical conductivities and magnetic properties.[15,16] It was found that PANI or PPy coating on BF NPs substantially reinforced the reflection loss of barium ferrite in 2−18 GHz. A recent paper on Ni/PANI core/shell nanocomposites indicated that an enhanced interfacial relaxation occurred by constructing a complete core−shell-type Ni/PANI nanocomposites and a multiloss combination contributed to enhanced microwave absorption.[10] It is believed that the complex permittivity ($\epsilon_r = \epsilon' + i\epsilon''$), permeability ($\mu_r = \mu' + i\mu''$), the electromagnetic impedance matching, and the structure of the absorber will all affect the microwave absorbing properties.[17]

In this article, selecting PPy as the conducting polymer, electromagnetic functionalized Ni/PPy microstructured core/shell composites were prepared by a conventional in situ chemical oxidative polymerization. To avoid strong reaction of Ni powder and acid, a weak acid, citric acid ($C_6H_8O_7$), was chosen as the dopant. It is understood that the content of the PPy can significantly affect the magnetic and electromagnetic properties of the resulting Ni/PPy composites.

Experimental Section

Synthesis of Ni/PPy Composites. Ni powder was bought from Fluka Chemika and used as received. The Ni/PPy composites were synthesized by an in situ chemical oxidative polymerization in the presence of Ni powders, with APS as oxidant and citric acid ($C_6H_8O_7$) as dopant. A typical preparation process for Ni/PPy composites is as follows: Ni powders were

* Corresponding author. Telephone: +86-451-86413702. Fax: +86-451-86418750. E-mail: pingxu_hit@yahoo.com.cn.
† Department of Applied Chemistry, Harbin Institute of Technology.
‡ Beijing Institute of Aeronautical Materials.

10.1021/jp804327k CCC: $40.75
Published on Web 08/06/2008

added to 0.2 M $C_6H_8O_7$ solution under ultrasonication for 30 min to obtain a uniform suspension, and then pyrrole monomer was added under ultrasonication for another 30 min to form a pyrrole/$C_6H_8O_7$ mixture containing Ni powder. The mixture was cooled in an ice−water bath for 1 h before adding precooled APS aqueous solution for oxidative polymerization for 12 h under vigorous mechanical stirring, with the temperature controlled at 0−5 °C. The precipitated powder was centrifugalized and washed with distilled water and anhydrous ethanol till the filtrate became colorless and then dried in a vacuum drying cabinet at 80 °C for 24 h. Throughout the experiment, the molar ratios of pyrrole to $C_6H_8O_7$ ([pyrrole]:[$C_6H_8O_7$]) and to APS ([pyrrole]:[APS]) were retained both at 1:1. Effects of the concentration of Ni powder on the morphology, structure, and physicochemical properties of the resulting Ni/PPy composites were studied by modulating mass ratios of Ni powder to pyrrole monomer (Ni/Py) at 4:1, 2:1, 1:1, and 1:2, respectively. Pure PPy was prepared under the same conditions without Ni powder.

Characterization. The morphologies of the samples were characterized by scanning electron microscopy (SEM, JEOL JSM-6701F) and transmission electron microscopy (TEM, TECNAI G^2 T20 S-TWIN). The characteristics of the crystallite structure of the prepared samples were determined using an XRD-6000 X-ray diffractometer (Shimadzu) with a Cu Kα radiation source ($\lambda = 1.5405$ Å, 40.0 kV, 30.0 mA). The Fourier transform infrared (FT-IR) spectroscopy was measured on Nicolet Avatar 360 FT-IR Spectrometric Analyzer with KBr pellets. The thermogravimetric (TG) analysis was carried out on a SETSYS Evolution TGA (Setaram) in the temperature range of room temperature to 1000 °C using a heating rate of 10 °C min^{-1}. The electrical conductivity of compressed rods at room temperature was measured by a standard four-probe method using a Keithley 2400 System digital sourcemeter. The magnetic properties (intrinsic coercivity, saturation and remanent magnetization) were measured using a vibrating sample magnetometer (VSM, Lake Shore 7307). A HP-5783E vector network analyzer was applied to determine the relative permeability and permittivity in the frequency range of 2−18 GHz for the calculation of reflection loss. A sample containing 50 wt % of obtained prodcuts was pressed into a ring with an outer diameter of 7 mm, an inner diameter of 3 mm, and a thickness of 2 mm for microwave measurement, in which paraffin wax was used as the binder.

Results and Discussion

As shown in Figure 1a, SEM image of commercially bought Ni powder displays micrometer Ni sphere-like and flower-like structures, which are in fact conglomerates of smaller and irregular Ni blocks. The formation of such microstructures may be explained by the strong magnetic attraction of the ferromagnetic Ni samples. As reported, preparation of PPy from a conventional chemical oxidative polymerization of pyrrole without any surfactant yielded microstructured PPy quasi-spheres.[16,18] Here, with citric acid as dopant, overlapped quasi-spherical PPy powders with an average diameter of about 0.3 μm was produced (Figure 1b). By polymerization of pyrrole monomers in the presence of Ni powder, it is interestingly found that the produced Ni/PPy composites all possess sphere-like structures, and no structures corresponding to Ni powder were distinguished (Figure 1c−f), which indicates that the Ni powders are uniformly coated with PPy, and thus fully core/shell structures are produced for Ni/PPy microstructured composites. It can be seen that the sizes of individual Ni/PPy spheres from overlapped

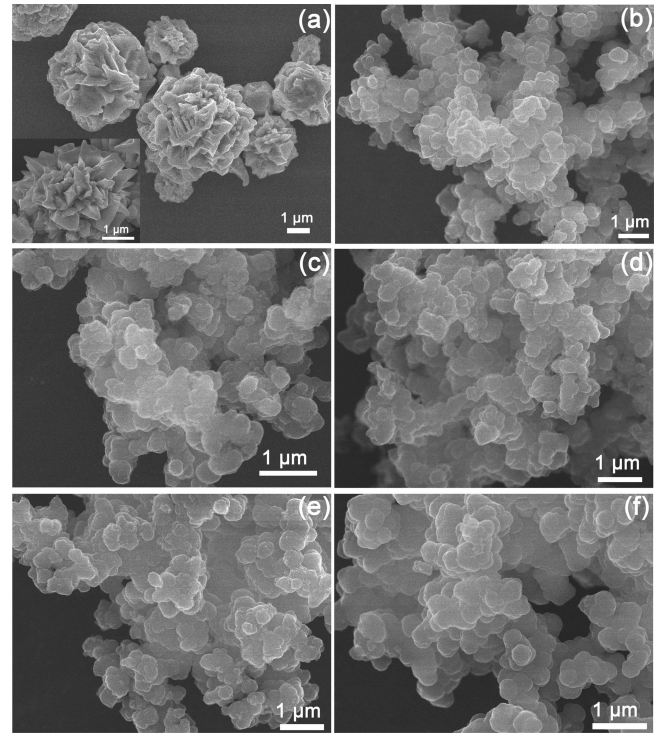

Figure 1. SEM images of (a) Ni powder, (b) protonated PPy, and Ni/PPy composites synthesized from different mass ratios of pyrrole monomer and Ni powder at (c) Ni/Py = 4:1, (d) Ni/Py = 2:1, (e) Ni/Py = 1:1, and (f) Ni/Py = 1:2 by an in situ chemical oxidative polymerization.

structures are in the range of 0.35−0.5 μm, which are much smaller than those of Ni conglomerates, indicating that Ni conglomerates are well dispersed during the chemical oxidative polymerization of pyrrole in an aqueous acidic solution medium. With the increase in the PPy content in Ni/PPy composites, a slight increase in the diameters of the spherical structures is observed, which is due to the increasing thickness of the PPy shells. It is found in a typical TEM photo of Ni/PPy with Ni/Py = 1:1 that the encapsulated Ni can diversify in sizes and morphologies: sphere-like Ni conglomerates with sizes of about 250−300 nm and Ni nanoflakes with sizes less than 100 nm can both be distinguished. Combined with SEM images, we think multiple nanocrystals of Ni can be encapsulated in the Ni/PPy microspheres.

Figure 2 shows the X-ray diffraction (XRD) patterns for Ni powder and Ni/PPy composites. In Figure 2a, the diffraction peaks at $2\theta = 44.5$, 51.8, and 76.4° can be well indexed to the (111), (200), and (220) planes of cubic fcc-type Ni crystals (JCPDS 65−2865). As for Ni/PPy composites (Figure 2b−e), the diffraction peaks of Ni crystals can be clearly distinguished for all the samples, while the diffraction intensities of the three peaks decrease with the reduction of the content of Ni powder. From the magnified XRD patterns at $2\theta = 10-40°$ (inset in Figure 2), a broad amorphous diffraction peak centered at around $2\theta = 24°$ was discovered for Ni/PPy composites, corresponding to the scattering from bare polymer chains at the interplanar spacing of protonated PPy.[19] It has been reported that the structure of polypyrroles doped with common counterions are essentially amorphous. Moreover, it is well-known that during the chemical synthesis of PPy, α−α′ bonds are predominantly formed, but a small proportion of α−β bonds are also present, leading to structural disorder (branching, cross-links) and hence resulting in an amorphous PPy.[16] As shown, with the increase in the content of Ni powder in Ni/PPy composites, the broad

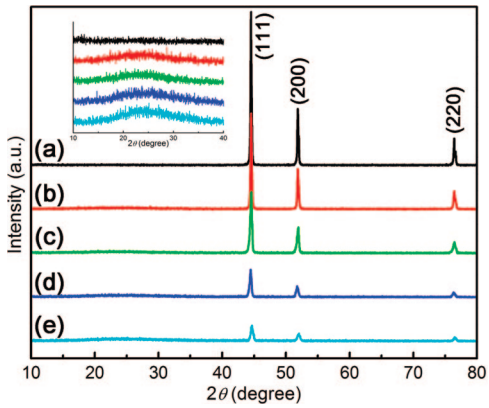

Figure 2. X-ray diffraction (XRD) patterns of (a) Ni powder, (b) Ni/Py = 4:1, (c) Ni/Py = 2:1, (d) Ni/Py = 1:1, and (e) Ni/Py = 1:2. Inset: Magnified XRD patterns from $2\theta = 10-40°$.

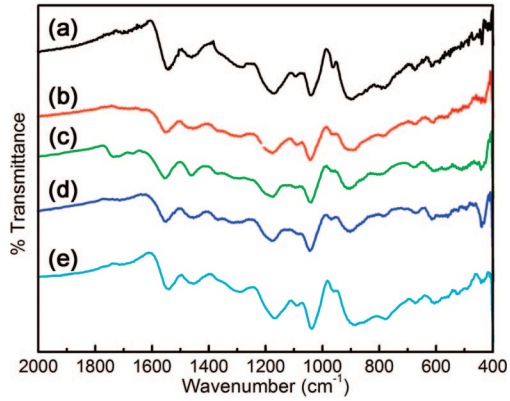

Figure 3. FT-IR spectra of (a) protonated PPy, (b) Ni/Py = 4:1, (c) Ni/Py = 2:1, (d) Ni/Py = 1:1, and (e) Ni/Py = 1:2.

amorphous diffraction peak of PPy becomes weaker, while the diffraction peaks corresponding to Ni crystals become much stronger.

FT-IR spectra of the prepared protonated PPy and Ni/PPy composites are displayed in Figure 3. For protonated PPy (Figure 3a), the bands observed at 1541 and 1459 cm^{-1} relate to the fundamental vibrations of the pyrrole rings.[20] The broadband from 1400 to 1250 cm^{-1} is attributed to the =C−H in-plane deformation modes, with a maximum at 1280 cm^{-1}. In the region of the C−N stretching vibrations from 1250 to 1100 cm^{-1}, one can observe a maximum at 1170 cm^{-1} in the spectra. The peak observed at 1093 cm^{-1} corresponds to the in-plane deformation vibration of NH^+, which is formed on the PPy chains by protonation.[21] The bands corresponding to the C−H and N−H in-plane deformation vibration situated at 1040 cm^{-1} and to the C−C out-of-plane ring deformation vibration at 963 cm^{-1}.[22] The region of the C−H out-of-plane deformation vibration of the ring locates at 899 cm^{-1} and the C−H out-of-plane ring deformation vibration at 792 cm^{-1}.[21] The peak at 675 cm^{-1} refers to the C−C out-of-plane ring deformation vibration or the C−H rocking vibration. The as-prepared Ni/PPy composites (Figure 3b−e) have identical characteristic vibrations for protonated PPy, and it can be discovered that the characteristic vibration peaks found for Ni/PPy composites almost have no shifts as compared with those for protonated PPy. XRD and FT-IR analyses may indicate that there is no obvious chemical interaction between Ni cores and PPy shells in the composites,[15,16,23] but that Ni powder only serve as the nucleation centers for the polymerization of pyrrole.

From the thermogravimetric (TG) curves (room temperature to 1000 °C) of the prepared protonated PPy, Ni powder and

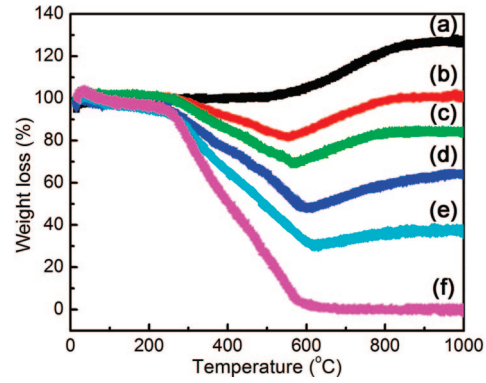

Figure 4. Thermogravimetric curves of the prepared (a) Ni powder, (b) Ni/Py = 4:1, (c) Ni/Py = 2:1, (d) Ni/Py = 1:1, (e) Ni/Py = 1:2, and (f) protonated PPy from room temperature to 1000 °C.

Ni/PPy composites shown in Figure 4, two weight loss regions and one weight increase region are discovered for the Ni/PPy composites, due to the removal of surface adsorbed water, the combustion of PPy (weight losses) and the reaction of Ni with O_2 to give NiO (a weight increase of 27.2% as shown in Figure 4a). It is noticed that the starting weight loss temperature of Ni/PPy composites due to the combustion of PPy locates at the same value as that of pure PPy, which may again verify that there's no chemical interaction between Ni powder and PPy. The mass percentage of PPy (x) in Ni/PPy composites can be calculated from the remanent weight percentage (W_R, wt %) and the weight loss due to the removal of adsorbed water (W_{water}, wt %) as follows:

$$(1 - x - W_{water})\frac{M(\mathrm{NiO})}{M(\mathrm{Ni})} = W_R \qquad (1)$$

Here M(NiO) and M(Ni) are the molar masses of NiO and Ni respectively. By this method, it is calculated that the real mass percentage of PPy in the Ni/PPy composites synthesized from designed mass ratios of Ni and pyrrole monomer (Ni/Py) at 4:1, 2:1, 1:1, and 1:2 are 20.4, 34.0, 48.5, and 65.7 wt % respectively, which conforms well to the mass ratios of Ni and PPy in Ni/PPy composites as designed.

It is well-known that the surface chemistry greatly affects the magnetic properties of fine magnetic particles due to their relatively larger surface area.[24] A comparative measurement of room-temperature field-dependent magnetic properties of protonated PPy, Ni powder and Ni/PPy composites was shown in Figure 5. For Ni powders, the saturation magnetization (M_S) and remanent magnetization (M_R) are 55.9 and 1.75 emu/g^{-1} respectively, with a coercivity of 36.2 Oe, which indicates a typical soft and ferromagnetic material. However, due to the dominant diamagnetic nature of PPy (inset in Figure 5) and the reduction of content of Ni powder, coating of PPy on Ni powders regularly reduces the M_S and M_R, and a linear increase relationship between M_S (M_R) and content of Ni powder was found for Ni/PPy composites. The M_S (M_R) for Ni/PPy composites with Ni/Py = 4:1, 2:1, 1:1, and 1:2 are 44.1 (1.26), 33.8 (0.94), 25.6 (0.79), and 16.5 (0.50) emu g^{-1}, respectively. It is interestingly found that the coercivities of Ni/PPy composites are almost the same as that of Ni powder (≈36 Oe), therefore, the as-prepared Ni/PPy composites are also soft and ferromagnetic materials.

Figure 6 shows the real part (μ') and imaginary part (μ'') of the relative complex permeability of the Ni powder and Ni/PPy composites, where the μ' values of Ni powder exhibit an abrupt decrease from 1.13 to 0.8 in the 2−12 GHz and retain

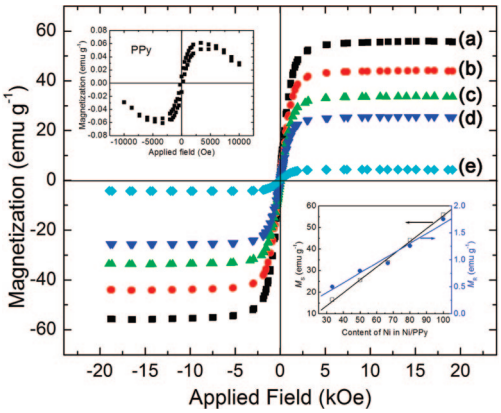

Figure 5. Room-temperature field-dependent magnetization curves of (a) Ni powder, (b) Ni/Py = 4:1, (c) Ni/Py = 2:1, (d) Ni/Py = 1:1, (e) Ni/Py = 1:2, and protonated PPy (inset: upper left). The relationship between M_S (M_R) and content of Ni powder in Ni/PPy is also displayed (inset: lower right).

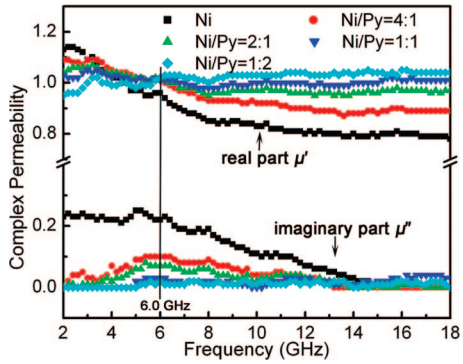

Figure 6. Real (μ') and imaginary (μ'') parts of the relative complex permeability of Ni powder and Ni/PPy composites in the frequency range of 2−18 GHz.

an approximate constant over 12−18 GHz. The μ' of Ni/PPy composites are higher than those of Ni powder in 4.6−18 GHz frequency range and present an intersecting point at 6.0 GHz, implying a normal resonance phenomenon. It is discovered that before the intersecting point, higher μ' values are found for Ni/PPy composites containing more Ni powder, while inverse changes are distinguished after the intersecting point. Meanwhile, the μ'' of the Ni/PPy composites are uniformly smaller than those of Ni powder in the whole range of 2−18 GHz, and it is interestingly found that broad peaks centered at 6.0 GHz are present in Ni/PPy composites, confirming that the natural resonance occurred in the prepared Ni/PPy composites. Compared with the fcc-type bulk Ni (several tens of megahertz),[10] the higher natural resonance frequency can be attributed to a larger surface anisotropic field due to the PPy coating and reduction in size. It is expected that the natural resonance will result in strong magnetic loss abilities, implying enhanced electromagnetic absorption during gigahertz frequency ranges.

The real part (ϵ') and imaginary part (ϵ'') of the relative complex permittivity represent the energy storage ability and loss ability respectively, and Figure 7 shows ϵ'' and ϵ'' of the Ni powder and Ni/PPy composites in the frequency range of 2−18 GHz. The ϵ' and ϵ'' of Ni powder are almost constant with nearly no variation throughout the whole frequency range ($\epsilon' \approx 7.4$, $\epsilon'' \approx 0.55$), indicating very poor dielectric loss. For Ni/PPy composites with Ni/Py = 4:1, 2:1, 1:1, and 1:2, the ϵ' values decrease from 17.1, 15.9, 23.1, and 35.0 to 8.6, 6.8, 8.7, and 14.3 in the 2−18 GHz range, respectively; while the ϵ'' decrease from 8.5, 11.6, 24.7, and 25.3 to 5.1, 4.1, 6.6, and

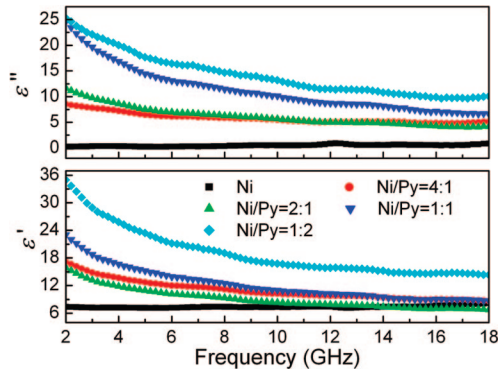

Figure 7. Real (ϵ') and imaginary (ϵ'') parts of the relative complex permittivity of Ni powder and Ni/PPy composites in the frequency range of 2−18 GHz.

9.8, respectively. According to the free electron theory,[17] $\epsilon'' \approx 1/\rho\omega\epsilon_0$, where ω, ϵ_0, and ρ are the angular frequency, the dielectric constant of free space, and the resistivity, respectively, from which it can be speculated Ni/Py = 4:1 and 2:1 have higher electric resistivity than Ni/Py = 1:1 and 1:2. Measurements of the electrical conductivities confirm that Ni/PPy composites with more PPy components have higher electrical conductivities, i.e., lower electrical resistivities. It can be seen both ϵ' and ϵ'' are obviously enhanced by coating Ni powder with PPy shells, which plays a dominant role in determining the dielectric loss properties. However, it should be pointed out that high electric resistivity and proper dielectric loss are favorable to improving the electromagnetic absorption properties.

According to the Debye dipolar relaxation, the complex permittivity (ϵ_r) can be written as[25]

$$\varepsilon_r = \varepsilon' + i\varepsilon'' = \varepsilon_\infty + \frac{\varepsilon_s - \varepsilon_\infty}{1 + i\omega\tau_0} \tag{2}$$

where τ_0, ϵ_s, and ϵ_∞ are the relaxation time, the static dielectric constant, and the dielectric constant at infinite frequency, respectively. From eq 2, it can be deduced that

$$\varepsilon' = \varepsilon_\infty + \frac{\varepsilon_s - \varepsilon_\infty}{1 + (\omega\tau_0)^2} \tag{3}$$

$$\varepsilon'' = \frac{\omega\tau_0(\varepsilon_s - \varepsilon_\infty)}{1 + (\omega\tau_0)^2} \tag{4}$$

It can be further deduced from eqs 3 and 4 that

$$(\varepsilon' - \varepsilon_\omega)^2 + (\varepsilon'')^2 = (\varepsilon_s - \varepsilon_\omega)^2 \tag{5}$$

Thus the plot of ϵ'' versus ϵ' would be a single semicircle, which is usually defined as the Cole−Cole semicircle.[26] Plots of ϵ'' versus ϵ' for Ni/PPy composites are shown in Figure 8, where three superimposed Cole−Cole semicircles are found for all the four samples, as Barthel, et al. found in alcohols,[27] which may suggest that there are ternary dielectric relaxation processes, with each semicircle corresponding to a Debye dipolar relaxation. Under a sufficient electromagnetic field, electrons that reside on the nitrogen atoms of the PPy may gain enough energy to surmount the interface between the PPy and the Ni powder and move onto the Ni particles, and thus an interfacial behavior of accumulating space charges is expected for Ni/PPy composites, as proposed in Ni/PANI and Au/PANI nanocomposites.[5,10,28] Meanwhile, acid doping endows the protonated PPy with permanent electric dipoles by introducing new hopping centers, leading to a steady dielectric relaxation. Furthermore, besides

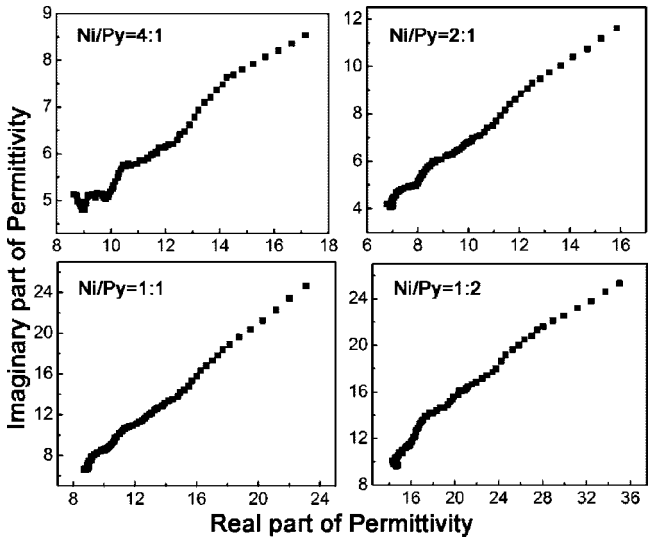

Figure 8. Typical Cole−Cole semicircles (ϵ'' versus ϵ') for Ni/PPy composites in the frequency range of 2−18 GHz.

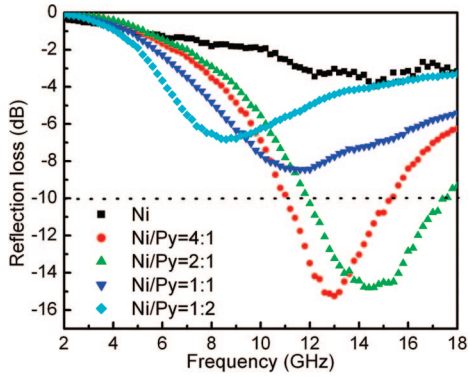

Figure 9. Reflection loss for Ni/PPy composites and Ni powder, with a sample thickness of 2 mm in the frequency range of 2−18 GHz. In measurement, 50 wt % sample and 50 wt % paraffin wax were used.

the enhanced dielectric relaxation of the PPy shells, an interfacial relaxation is present because a core/shell interface is formed by coating Ni powder with PPy shells. Debye-type dielectric relaxation is absent for the metallic Ni powders, thus the ternary dielectric relaxation processes are mainly induced by the PPy coatings, which is expected to result in enhanced dielectric loss.

To further prove the dependence of the microwave absorption properties on the complex permittivity and complex permeability, the reflection loss properties [R(dB)] of Ni powder and Ni/PPy composites were calculated from the transmission line theory,[29] as

$$R(\mathrm{dB}) = 20 \log\left|\frac{Z_{\mathrm{in}} - 1}{Z_{\mathrm{in}} + 1}\right| \tag{6}$$

Z_{in} is the normalized input impedance of a metal-backed microwave-absorbing layer

$$Z_{\mathrm{in}} = \sqrt{\frac{\mu_{\mathrm{r}}}{\varepsilon_{\mathrm{r}}}} \tanh\left[j\left(\frac{2\pi}{c}\right)\sqrt{\mu_{\mathrm{r}}\varepsilon_{\mathrm{r}}} f d\right] \tag{7}$$

where c is the velocity of electromagnetic waves in free space, f is the frequency of microwaves, and d is the thickness of the absorber. Figure 9 shows the reflection loss of the Ni powder and the prepared Ni/PPy composites with a thickness of 2 mm in the frequency range of 2−18 GHz, which displays that the reflection loss characteristics are sensitive to the content of PPy in Ni/PPy composites. With poor dielectric loss, the reflection loss properties of Ni powder are expected mainly from magnetic loss, with a minimum reflection loss of −4 dB at 14.4 GHz. It can be observed that the reflection loss properties toward electromagnetic waves of Ni/PPy composites were enhanced substantially, as compared to those of pure Ni powder. The frequency relating to minimum reflection loss can be modulated by altering the content of PPy in Ni/PPy composites, and the increased reflection loss at higher frequency range is accompanied by the attenuation at lower frequency bands. The minimum reflection losses of Ni/PPy composites from Ni/Py = 4:1, 2:1, 1:1, and 1:2 are −15.2, −14.8, −8.4, and −6.8 dB at 13.0, 14.4, 11.6, and 8.6 GHz respectively, and electromagnetic absorption less than −10 dB is only found for Ni/Py = 4:1 and 2:1, in the 11−15.4 GHz range for the former and 12−17.5 GHz for the latter. The electromagnetic absorption properties of Ni/PPy composites from Ni/Py = 4:1 and 2:1 are much better than those of Ni/PANI nanocomposites and $BaTiO_3$/PANI composites at the same thickness in the frequency range of 2−18 GHz.[10,12] As shown from complex permittivity, higher ϵ'' for Ni/Py = 1:1 and 1:2, or to say, lower electrical resistivity, is not beneficial to enhanced microwave absorption. Enhanced microwave absorption of core/shell micro/nanostructures has been reported due to the lag of polarization between the core/shell interfaces,[17] and it is evident that there is interfacial relaxation between Ni cores and PPy shells. A natural resonance at 6.0 GHz was found for Ni/PPy composites from the complex permeability, while no reflection loss peaks are present at this frequency. As found in previous papers,[15,16] besides the complex relative permeability μ_{r} and permittivity ϵ_{r}, another important parameter relating to reflection loss is the concept of matched characteristic impedance, where the characteristic impedance of the absorbing material should be made nearly equal to that of the free space to achieve zero reflection at the front surface of the material.[30] Therefore, the ternary Debye relaxations for enhanced dielectric loss induced by PPy coatings and proper electromagnetic impedance matching due to the synergetic consequence of the Ni cores and PPy shells are critical to the improvement of the electromagnetic absorption of the Ni/PPy core/shell composites. In preparation of dielectric materials for electromagnetic wave absorption, one should simultaneously consider the dielectric loss and electrical conductivity of such materials in order to achieve optimum reflection loss properties.

Conclusions

With Ni powders as nucleation centers, electromagnetic functionalized core/shell Ni/PPy microstructured composites were synthesized from an in situ chemical oxidative polymerization, and it is proved by XRD and FT-IR that there's no obvious chemical interaction between the Ni cores and PPy shells. The Ni/PPy composites are soft and ferromagnetic materials, and a linear increase of saturation magnetization and remanent magnetization as a function of Ni powder content is displayed, where the coercivities remain nearly unchanged. Compared with the bulk Ni, a higher natural resonance frequency at 6.0 GHz found in all Ni/PPy composites can be attributed to a larger surface anisotropic field due to the PPy coating and reduction in size. Both ϵ' and ϵ'' are obviously enhanced by coating Ni powder with PPy shells, and ternary dielectric relaxation processes are found from Cole−Cole semicircle approach. The ternary Debye relaxations for enhanced dielectric loss induced by PPy coatings and proper electromagnetic impedance matching due to the synergetic consequence

of the Ni cores and PPy shells contribute to the enhanced electromagnetic absorption of the Ni/PPy core/shell composites.

Acknowledgment. P.X. thanks Shufa Zheng for SEM measurements. This work is supported by the NSF of China (No. 20676024, 20776032) and Innovative Foundation of Heilongjiang Academy of Sciences (HKXY-CX-07001-03).

Supporting Information Available: Figures showing plots of ϵ'' versus ϵ' for Ni powder, TEM, and electrical conductivity of Ni/PPy. This material is available free of charge via the Internet at http://pubs.acs.org.

References and Notes

(1) Lo, M. Y.; Zhen, C.; Lauters, M.; Jabbour, G. E.; Sellinger, A. *J. Am. Chem. Soc.* **2007**, *129*, 5808.

(2) Rickert, P. G.; Antonio, M. R.; Firestone, M. A.; Kubatko, K.-A.; Szreder, T.; Wishart, J. F.; Dietz, M. L. *J. Phys. Chem. B* **2007**, *111*, 4685.

(3) Sawall, D. D.; Villahermosa, R. M.; Lipeles, R. A.; Hopkins, A. R. *Chem. Mater.* **2004**, *16*, 1606.

(4) Watanabe, N.; Morais, J.; Accione, S. B. B.; Morrone, Â.; Schmidt, J. E.; Martins Alves, M. C. *J. Phys. Chem. B* **2004**, *108*, 4013.

(5) Tseng, R. J.; Huang, J.; Ouyang, J.; Kaner, R. B.; Yang, Y. *Nano Lett.* **2005**, *5*, 1077.

(6) Pillalamarri, S. K.; Blum, F. D.; Tokuhiro, A. T.; Bertino, M. F. *Chem. Mater.* **2005**, *17*, 5941.

(7) Feng, X.; Huang, H.; Ye, Q.; Zhu, J.; Hou, W. *J. Phys. Chem. C* **2007**, *111*, 8463.

(8) Gomez-Romero, P. *Adv. Mater.* **2001**, *13*, 163.

(9) Wuang, S. C.; Neoh, K. G.; Kang, E. T.; Pack, D. W.; Leckband, D. E. *J. Mater. Chem.* **2007**, *17*, 3354.

(10) Dong, X. L.; Zhang, X. F.; Huang, H.; Zuo, F. *Appl. Phys. Lett.* **2008**, *92*, 013127.

(11) Kazantseva, N. E.; Vilcakova, J.; Kresalek, V.; Saha, P.; Sapurina, I.; Stejskal, J. *J. Magn. Magn. Mater.* **2004**, *269*, 30.

(12) Abbas, S. M.; Dixit, A. K.; Chatterjee, R.; Goel, T. C. *Mater. Sci. Eng., B* **2005**, *123*, 167.

(13) Selvan, S. T.; Spatz, J. P.; Klok, H.; Möller, M. *Adv. Mater.* **1998**, *10*, 132.

(14) Tian, S.; Liu, J.; Zhu, T.; Knoll, W. *Chem. Mater.* **2004**, *16*, 4103.

(15) Xu, P.; Han, X.; Jiang, J.; Wang, X.; Li, X.; Wen, A. *J. Phys. Chem. C* **2007**, *111*, 12603.

(16) Xu, P.; Han, X.; Wang, C.; Zhao, H.; Wang, J.; Wang, X.; Zhang, B. *J. Phys. Chem. B* **2008**, *112*, 2775.

(17) Zhang, X. F.; Dong, X. L.; Huang, H.; Liu, Y. Y.; Wang, W. N.; Zhu, X. G.; Lv, B.; Lei, J. P.; Lee, C. G. *Appl. Phys. Lett.* **2006**, *89*, 053115.

(18) Zhong, W.; Liu, S.; Chen, X.; Wang, Y.; Yang, W. *Macromolecules* **2006**, *39*, 3224.

(19) Seo, I.; Pyo, M.; Cho, G. *Langmuir* **2002**, *18*, 7253.

(20) Nguyen, T.; Diaz, A. *Adv. Mater.* **1994**, *6*, 858.

(21) Blinova, N. V.; Stejskal, J.; Trchová, M.; Prokeš, J.; Omastová, M. *Eur. Polym. J.* **2007**, *43*, 2331.

(22) Şen, S.; Gök, A.; Gülce, H. J. *Appl. Polym. Sci.* **2007**, *106*, 3852.

(23) Zhang, L.; Wan, M. J. *Phys. Chem. B* **2003**, *107*, 6748.

(24) Yavuz, Ö.; Ram, M. K.; Aldissi, M.; Poddar, P.; Hariharan, S. *J. Mater. Chem.* **2005**, *15*, 810.

(25) Fang, P. H. *J. Chem. Phys.* **1965**, *42*, 3411.

(26) Cole, K. S.; Cole, R. H. *J. Chem. Phys.* **1941**, *19*, 1484.

(27) Barthel, J.; Bachhuber, K.; Buchner, R.; Hetzenauer, H. *Chem. Phys. Lett.* **1990**, *165*, 369.

(28) Tseng, R. J.; Cunha, H. N. D.; Faria, R. M.; Huang, J. X.; Kaner, R. B.; Ouyang, J. Y.; Yang, Y. *Appl. Phys. Lett.* **2007**, *90*, 053101.

(29) Singh, P.; Babbar, V. K.; Razdan, A.; Puri, R. K.; Goel, T. C. *J. Appl. Phys.* **2000**, *87*, 4362.

(30) Vinoy, K. J.; Jha, R. M. *Radar Absorbing Materials: From Theory to Design and Characterization*; Kluwer Academic Publishers: Dordrecht, The Netherlands, 1996.

JP804327K